Title

Cartilage T1ρ and T2 relaxation times: longitudinal reproducibility and variations using different coils, MR systems and sites

Journal

Osteoarthritis and Cartilage, 23(12)

ISSN

1063-4584

Authors

Li, X
Pedoia, V
Kumar, D
et al.

Publication Date

2015-12-01

DOI

10.1016/j.joca.2015.07.006

Peer reviewed

HHS Public Access

Author manuscript

Osteoarthritis Cartilage. Author manuscript; available in PMC 2016 December 01.

Published in final edited form as:

Osteoarthritis Cartilage. 2015 December ; 23(12): 2214–2223. doi:10.1016/j.joca.2015.07.006.

Cartilage $T_{1\rho}$ and T_2 relaxation times: Longitudinal reproducibility and variations using different coils, MR systems and sites

Xiaojuan Li, PhD[1], **Valentina Pedoia, PhD**[1], **Deepak Kumar, PT, PhD**[1], **Julien Rivoire, PhD**[1], **Cory Wyatt, PhD**[1], **Drew Lansdown, MD**[1], **Keiko Amano, MD**[1], **Narihiro Okazaki, MD**[1], **Dragana Savic, MS**[1], **Matthew F. Koff, PhD**[2], **Joel Felmlee, PhD**[3], **Steven L. Williams, MS**[3], and **Sharmila Majumdar, PhD**[1]

[1]University of California, San Francisco, CA, USA

[2]Hospital for Special Surgery, New York, NY, USA

[3]Mayo Clinic, Rochester MN, USA

Abstract

OBJECTIVE—To evaluate the longitudinal reproducibility and variations of cartilage $T_{1\rho}$ and T_2 measurements using different coils, MR systems and sites.

METHODS—Single-Site study: Phantom data were collected monthly for up to 29 months on four GE 3T MR systems. Data from phantoms and human subjects were collected on two MR systems using the same model of coil; and were collected on one MR system using two models of coils. Multi-site study: Three participating sites used the same model of MR systems and coils, and identical imaging protocols. Phantom data were collected monthly. Human subjects were scanned and rescanned on the same day at each site. Two traveling human subjects were scanned at all three sites.

RESULTS—Single-Site Study: The phantom longitudinal RMS-CVs ranged from 1.8% to 2.7% for $T_{1\rho}$ and 1.8% to 2.8% for T_2. Significant differences were found in $T_{1\rho}$ and T_2 values using different MR systems and coils. Multi-Site Study: The phantom longitudinal RMS-CVs ranged from 1.3% to 2.6% for $T_{1\rho}$ and 1.2% to 2.7% for T_2. Across three sites (n=16), the *in-vivo* scan-rescan RMS-CV was 3.1% and 4.0% for $T_{1\rho}$ and T_2, respectively. Phantom $T_{1\rho}$ and T_2 values were significantly different between three sites but highly correlated (R>0.99). No significant

Corresponding Author: Xiaojuan Li, PhD, Associate Professor, Department of Radiology, University of California at San Francisco, 185 Berry Street, Suite 350, San Francisco, CA. 94107, Tel: (415) 353-4909, Fax: (415) 353-9423, xiaojuan.li@ucsf.edu.

Author Contributions

Study and Concept Design: XL, SM
Data Collection and Coordination: VP, DK, JR, CW, DL, DS, MFK, JF, SLW
Data Analysis and Results Interpretation: XL, VP, DK, JR, CW, DL, NO, KA
Manuscript Draft: XL
Critical Review, Edit and Proof of Manuscript: all authors

Conflict of Interest

No conflict of interest to the study from all authors.

difference was found in $T_{1\rho}$ and T_2 values of traveling controls, with cross-site RMS-CV as 4.9% and 4.4% for $T_{1\rho}$ and T_2, respectively.

CONCLUSION—With careful quality control and cross-calibration, quantitative MRI can be readily applied in multi-site studies and clinical trials for evaluating cartilage degeneration.

Keywords

Cartilage; Quantitative MRI; $T_{1\rho}$; T_2; Reproducibility; Multi-site study

INTRODUCTION

Osteoarthritis (OA) constitutes a significant health burden affecting more than 27 million people in US alone (1, 2), and has been recognized as one of the fastest growing medical conditions world wide due to the increased prevalence of obesity and aging of society (3). The disease is characterized primarily by cartilage degeneration. MR techniques that quantify cartilage matrix changes have become more accessible, with the rationale that detecting early and subtle cartilage degeneration would be critical for allowing early intervention, monitoring treatment efficacy, and leading to prevention strategies for OA (4–7). Among these techniques, $T_{1\rho}$ and T_2 relaxation time quantification have gained significant attention because they do not need contrast agent injection nor special hardware, and can be feasibly performed in a clinical setting. T_2 mapping is a product sequence while $T_{1\rho}$ mapping prototype acquisitions are available from all major MR manufacturers. Numerous studies have shown that $T_{1\rho}$ and T_2 quantification techniques can detect early cartilage damage and degeneration in patients with OA, acute joint injury or cartilage damage (8–16).

Despite the promising results, the application of $T_{1\rho}$ and T_2 quantification in multicenter clinical studies and trials is very limited. One impeding factor is the limited documentation of potential variations of $T_{1\rho}$ and T_2 by using different MR systems, coils, and sites (17–19). Furthermore, longitudinal assessment of cartilage degeneration requires reproducible quantitative measurements over time. Previous studies of $T_{1\rho}$ and T_2 reproducibility were primarily limited to short-term reproducibility, except for the 3- and 8-year T_2 data as part of the OA Initiative (OAI) study quality control (17, 18). Understanding and documenting these variations are critical for setting up multi-center longitudinal studies using $T_{1\rho}$ and T_2 techniques.

Currently, a multi-center feasibility study of applying $T_{1\rho}$ and T_2 quantification techniques in knees after acute ACL injury is being performed at three geographically remote centers. In this report, we first evaluated the longitudinal reproducibility and variations of $T_{1\rho}$ and T_2 values using different MR systems and coils at one site (a single-site study), and then evaluated the reproducibility and cross-validation results among three sites (the multi-site study).

METHODS

Study Design

The overall study design is illustrated in Figure 1, and is described in detail below in two sections: the single-site and multi-site study. This study was approved by the Committee for Human Research at all institutions participating in the study, and informed consent was obtained from all subjects prior to data acquisition.

Single-Site Study—The study was designed to evaluate: 1) short and long-term reproducibility of $T_{1\rho}$ and T_2 values; 2) the variation of $T_{1\rho}$ and T_2 values using different model MR systems from the same vendor; and 3) the variation of $T_{1\rho}$ and T_2 values using different coils. All the data were collected between September 2011 and July 2014.

To evaluate short-term and long-term reproducibility, phantoms were scanned monthly using three models of GE 3T MR systems (GE Healthcare, Milwaukee, WI) using knee coils of the same model from the same vendor (quadrature transmit/8-channel phased-array receive knee coil, InVivo, Gainesville, FL, termed as 'QT8PAR knee coil' below) at a single institution: GE Signa HDx long bore (maximum gradient strength: 50 mT/m; slew rate 150 mT/m/sec; bore size: 60 cm); GE MR750 (maximum gradient strength: 50 mT/m; slew rate 200 mT/m/sec; bore size: 60 cm); GE MR750 wide bore (maximum gradient strength: 44 mT/m; slew rate: 200mT/m/sec; bore size: 70 cm).

To evaluate the variation of $T_{1\rho}$ and T_2 values using different MR systems, phantom data was collected at four GE 3T MR systems at the same institution: the three MR systems above and a GE Signa HDx short bore (maximum gradient strength: 23 mT/m whole mode, 40 T/m zoom code; slew rate: 80 mT/m/sec whole mode, 150 mT/m/sec zoom mode; bore size: 60 cm). In addition, 10 healthy subjects were scanned on both the HDx long bore and the MR750 wide bore using the same model of QT8PAR knee coils within a period of 3-months.

To evaluate the variation of $T_{1\rho}$ and T_2 values using different coils, five healthy subjects were scanned on the MR750 wide bore using a QT8PAR knee coil and a 16-channel phased-array receive only flex coil (GE Healthcare, termed as '16PAR flex coil' below).

Multi-Site Study—All three sites used GE MR750 systems with QT8PAR knee coils. The study was designed to evaluate: 1) reproducibility of $T_{1\rho}$ and T_2 values in phantoms scanned monthly at each site; 2) scan/re-scan (on the same day) reproducibility of $T_{1\rho}$ and T_2 values in healthy controls at each site (n = 6, 5, 5 for site 1, 2, 3 respectively); and 3) cross-validation of $T_{1\rho}$ and T_2 values in the same phantom sets and in the same volunteers across three sites. For phantom scans, one phantom set was scanned at all three sites at one time point. For human subject scans, two volunteers travelled and were scanned at all three sites at baseline and at 10-month follow-up. At all three sites, the same sequence and same imaging protocol was used for both phantom and *in vivo* scans as detailed below. All of the data were collected between November 2013 and October 2014.

Imaging Protocol

Phantom Imaging Protocol—Phantoms were created by dissolving agarose powder in deionized water at different concentrations (weight/volume, 2%, 3%, 4%). Six phantom tubes (25 mm diameter, 2 for each concentration) were placed in a foam holder and named Phantoms #1-6. During each exam, phantoms were first scanned at isocenter, then left (70mm off-center), and right (70mm off-center) positions. At isocenter, $T_{1\rho}$ and T_2 measurements were acquired separately with 8 echoes each. At the left and right positions, $T_{1\rho}$ and T_2 measurements were acquired in a combined sequence with 4 echoes each (20) (Table 1).

In vivo Imaging Protocol—For the single-site study, the *in vivo* imaging protocol included high-resolution 3D fast spin-echo (FSE) images (CUBE) for cartilage segmentation, and $T_{1\rho}$ and T_2 sequences. $T_{1\rho}$ and T_2 measurements were acquired separately with 8-echoes each.

For the multi-site study, a custom leg-holder was used during data acquisition to ensure consistent knee flexion during scanning. The holders for all three sites were made from a common cast mold. The foot was positioned in a U-shaped foam holder (GE Healthcare, Milwaukee, WI) and oriented vertically to minimize any internal or external rotation of the knee joint. For this study, CUBE images were used for cartilage segmentation, the combined $T_{1\rho}$ and T_2 sequences were used with 4 echoes each, and additional fat-suppressed and non fat-suppressed 2D FSE images were collected for clinical evaluation of any joint damage (Table 1).

Image Analysis

All images were analyzed at one center under stringent quality control procedures. Acquisition parameters were first automatically checked to ensure consistency of imaging protocols, followed by visual evaluation of image quality (including orientation, coverage and artifacts) before quantitative analysis. Images with significant artifacts were excluded from analysis.

$T_{1\rho}$ and T_2 Quantification—The first step registered all *in vivo* images to the TSL=0 image to minimize motion between different echoes. For images acquired with separate $T_{1\rho}$ and T_2 sequences (8 TSLs for $T_{1\rho}$ and 8 TEs for T_2), $T_{1\rho}$ and T_2 maps were reconstructed by fitting the $T_{1\rho}$- and T_2-weighted images voxel-by-voxel to the equations below (three-parameter fitting):

$$S(TSL)=A\times\exp(-TSL/T_{1\rho})+B \quad (1)$$

$$S(TE)=A\times\exp(-TE/T_2)+B \quad (2)$$

For images acquired with combined $T_{1\rho}$ and T_2 sequence (4 TSLs for $T_{1\rho}$ and 4 TEs for T_2), $T_{1\rho}$ and T_2 maps were reconstructed by fitting the $T_{1\rho}$- and T_2-weighted images voxel-by-

voxel to the equations below (two-parameter fitting, because the three-parameter fitting would be suboptimal with only four echoes):

$$S(TSL)=A \times \exp(-TSL/T_{1\rho}) \quad (3)$$

$$S(TE)=A \times \exp(-TE/T_2) \quad (4)$$

For phantom images, an automatic program was applied to generate a circular ROI for each phantom in the middle four slices. The mean and standard deviation (SD) of $T_{1\rho}$ and T_2 relaxation times were calculated in ROIs for each phantom.

For *in vivo* data, the high resolution CUBE images were rigidly registered to the TSL = 0 images using the VTK CISG registration Toolkit. Cartilage was segmented semi-automatically using software developed in-house (21) on the registered CUBE images into six compartments: lateral/medial femur (LF/MF), the lateral/medial tibia (LT/MT), trochlea (TrR) and patella (P). The 3D regions of interest (ROIs) were then overlaid on the $T_{1\rho}$ and T_2 maps. The mean and SD $T_{1\rho}$ and T_2 values were calculated for each compartment.

SNR Calculation—In phantom scans, a second TSL = 0 image was acquired. The difference between the two TSL = 0 images was used for evaluating noise. SNR was calculated as the mean signal within phantom ROIs/SD of noise. *In vivo*, this analysis was not possible, instead the noise SD was estimated from the background region outside the knee and below the patella as proposed in reference (22). To limit the center-to-edge variability of SNR caused by a phased array receive coil, the center five slices were used in phantoms and the center four slices for medial and lateral femoral condyles were used in human subjects.

Statistical Analysis

The longitudinal and scan-rescan (short-term) reproducibility of $T_{1\rho}$ and T_2 values were evaluated using root-mean-square coefficients of variation (RMS-CV, %). The fitting errors were evaluated with RMS error normalized to the signal intensity of the TSL=0 image. The differences of $T_{1\rho}$ and T_2 values obtained at different positions (center vs. left vs. right) in the magnet, using different MR systems or different coils, and at different sites were evaluated using ANOVA, Bland-Altman, and pooled RMS analyses. Correlations between $T_{1\rho}$ and T_2 values within the subjects as well as correlations of $T_{1\rho}$ and T_2 values between MR systems were evaluated using the Spearman correlation coefficient R.

RESULTS

Single-Site Study

Long-term Reproducibility—Up to 29 months of data were collected from the three MR systems: HDx long bore (13 time points); MR750 (29 time points); MR750 wide bore (20 time points). Figure 2A and 2B shows the scatter plot of the $T_{1\rho}$ and T_2 at the magnet center position. Table 2A summarizes the RMS-CV of $T_{1\rho}$ and T_2 values at the center, left and right positions. Table 3 summarizes the number of voxels, mean $T_{1\rho}$ and T_2 values, pooled

SD and fitting errors within each phantom ROI, as well as the pooled RMS of inter-location variation and long-term reproducibility.

Variations in $T_{1\rho}$ and T_2 Values Using Different MR systems—In phantoms, $T_{1\rho}$ and T_2 values between any two MR systems were highly correlated (R > 0.9). However, significant differences were observed in $T_{1\rho}$ and T_2 values between MR systems (Figure 2C and 2D), with MR750 having the highest values relative to the other systems. The MR750 wide bore had significantly lower $T_{1\rho}$ values than HDx long bore (P=0.02, 95% CI (−3.1, −0.4)). However no significant difference in T_2 values were found between these two MR systems (P = 0.16, 95% CI (−0.2, 0.9)).

The HDx short bore had significantly higher SNR, and the MR750 wide bore had significantly lower SNR, compared to HDx long bore and MR750. For example, 3% agarose phantom images with TSL/TE= 0 had SNR 127.8, 89.9, 80.0 and 61.4 for HDx short bore, HDx long bore, MR750, MR750 wide bore, respectively.

The global *in vivo* cartilage $T_{1\rho}$ and T_2 values were significantly higher using HDx long bore compared to MR750 wide bore (34.3 ± 3.0 ms vs. 31.5 ± 2.9 ms, P = 0.00003, 95% CI (2.1, 3.5) for $T_{1\rho}$ and 25.2 ± 2.0 vs 22.3 ± 2.3 ms, P =0.002, 95% CI (1.5, 4.4) for T_2), (Figure 3A and 3B). $T_{1\rho}$ values between the two MR systems were highly correlated (R = 0.91) while T2 values were less well correlated (R = 0.64). The $T_{1\rho}$ and T_2 values within subjects using the same MR system were moderately correlated (R = 0.55) The *in vivo* SNR of $T_{1\rho}$- and T_2- weighted images were significantly higher using the HDx long bore compared to the MR750 wide bore (Table 4), in agreement with phantom results.

Variations in $T_{1\rho}$ and T_2 Values Using Different Coils—In phantoms, $T_{1\rho}$ and T_2 values were significantly higher using the 16PAR flex coil than those using the QT8PAR knee coil (P = 0.009, 95% CI = (0.4, 1.5) for $T_{1\rho}$; P = 0.02, 95% CI = (0.4, 3.0) for T_2). The difference in $T_{1\rho}$ was 0.6ms, 0.7ms and 1.6 ms, and the difference in T2 was 0.9ms, 1.7ms and 2.6ms for the 4%, 3% and 2% phantoms respectively. The SNR was significantly higher (the average SNR of TSL=0/TE=0 images was 165.7 vs. 97.0 for 16-channel and 8-channel coils respectively) while the fitting errors were significantly lower (the average fitting error was 0.0032 vs. 0.0054 for $T_{1\rho}$, 0.0037 vs. 0.0062 for T_2 for 16 channel and 8-channel coils respectively) using the 16PAR flex coil than those using the QT8PAR knee coil.

The global *in vivo* cartilage $T_{1\rho}$ and T_2 values were significantly higher using the 16PAR flex coil than those using the QT8PAR knee coil (32.9 ± 3.9 ms vs. 30.1 ± 3.1 ms, P =0.018, 95%CI (0.7, 3.6) for $T_{1\rho}$; 27.4 ± 1.8 vs. 23.4 ± 2.8, P = 0.012, 95% CI (1.7, 6.3) for T_2) (Figure 4A and 4B). No significant differences in fitting errors were observed between the two coils. The *in vivo* SNR of $T_{1\rho}$ - and T_2-weighted images using the 16PAR flex coil were significantly higher compared to using the QT8PAR knee coil (Table 4).

Multi-Site Study

Longitudinal Phantom Reproducibility—Table 2B summarizes the phantom RMS-CV for $T_{1\rho}$ and T_2 values of Site 1 (7 months), Site 2 (4 months) and Site 3 (8 months).

Scan-rescan Reproducibility of Healthy Controls at Each Site—Across all three sites (n=16), the scan-rescan RMS-CV was 3.1% and 4.0% for compartment $T_{1\rho}$ and T_2 values, respectively. The RMS-CV in each compartment ranged from 2.3% – 3.9% for $T_{1\rho}$, and ranged 3.2% – 5.3% for T_2 (Figure 5). Table 3 summarizes the number of voxels, mean $T_{1\rho}$ and T_2 values, pooled SD and fitting errors within each compartment, as well as the pooled RMS of scan-rescan (short-term) reproducibility.

Cross-validation of $T_{1\rho}$ and T_2 Values among Three Sites

In Phantoms: Phantom $T_{1\rho}$ and T_2 values were significantly different among the three sites but highly correlated ($R > 0.99$). The mean CV was 2.9% and 4.1% for $T_{1\rho}$ and T_2 values respectively.

In Healthy Controls: No significant differences were found in $T_{1\rho}$ and T_2 values in the traveling controls between the three sites, with 4.9% and 4.4% RMS-CV for $T_{1\rho}$ and T_2, respectively. No significant differences were found in $T_{1\rho}$ and T_2 values between baseline and 10-month follow-up, with 4.4% and 5.1% RMS-CV for $T_{1\rho}$ and T_2, respectively.

Table 3 summarizes the pooled $T_{1\rho}$ and T_2 RMS for phantoms and human subjects using the different MR systems, different coils, and different sites.

DISCUSSION

Quantitative evaluation of articular cartilage matrix composition using $T_{1\rho}$ and T_2 mapping can potentially provide early markers of cartilage degeneration. These methods, present significant challenges to make accurate measurements on a thin curved structure. This study evaluated the short and longitudinal reproducibility, as well as variations of $T_{1\rho}$ and T_2 values measured using different MR systems, coils and sites.

In our single-site study, the longitudinal RMS-CV of $T_{1\rho}$ and T_2 values were < 3% over periods from 13–29 months, indicating excellent longitudinal reproducibility. The T_2 results are in agreement with a multi site study with 1.7%–5.4% RMS-CV over an 8 year period (17). Factors that can introduce longitudinal variations of relaxation time measurements include any external variations of environment in the scanner room (temperature for example), MR system software or hardware upgrades, fluctuations in the MR system and coil performance, as well as changes in the phantom composition (primarily dehydration which will decrease $T_{1\rho}$ and T_2 values). In the present study, no obvious system drift was observed, suggesting that relaxation times can be measured reliably using modern MR systems over 29 months.

We observed significant differences in $T_{1\rho}$ and T_2 values between different models of MR systems and coils. The MR systems used in the single-site study had different hardware systems including peak gradient amplitude, gradient slew rate and bore size, which resulted in different pulse width and minimum TR/TE in $T_{1\rho}$ and T_2 sequences Also, the transmit gain differed and likely introduced flip angle variations. In addition, the coupling between the knee and body RF coils caused by the construction techniques as well as bone diameter

affects the efficiency of B_1, and flip angles, and SNR. All of these factors may affect relaxation time quantification.

The RF coil transmit uniformity, which is influenced by both coil design and electric loading with subjects, can be another key factor contributing to variations in relaxation time. In general, the body transmit provides more uniform RF fields compared to a local transmit coil, but deposits higher energy (SAR) and is thus restrictive. The transmit B_1 non-uniformity will introduce spatial variations in flip angles then in relaxation times. The QT8PAR knee coil used in this study however has been documented to have a fairly good transmit uniformity (22). In addition, the $T_{1\rho}$ and T_2 sequences used in the study applied composite hard pulses during magnetization preparation, which reduce the sensitivity to B_1 and B_0 inhomogeneity (20). Therefore, we do not anticipate the transmit uniformity to be an issue for the QT8PAR knee coil. In this study, higher SNR and higher $T_{1\rho}$ and T_2 values were observed using the 16PAR flex coil (with body coil transmit) compared to the QT8PAR knee coil. It was previously reported that the QT8PAR coil provided a higher SNR and increased T_2 values compared to a quadrature transmit/receive coil in the central MF and MT but not in the LT (22). The authors speculated the low SNR resulted in underestimated values, particularly in the deep cartilage with shorter T_2 values; however, the extent and significance of the difference was not consistent for all cartilage plates and depth (22) and may be caused by either physiology or B1 non-uniformity.

Based on our findings of significant differences in $T_{1\rho}$ and T_2 values for different model MR systems and coils, we allowed only GE MR750 3T MR systems with QT8PAR knee coils to be used in the multi-site post-ACL injury study. In addition, the identical $T_{1\rho}$ and T_2 sequence was used because different acquisition sequences can introduce significant differences in relaxation times (23). A custom leg-holder, with the foot was positioned vertically in a foot holder was used to ensure consistent flexion angles and minimize joint rotation during scanning. Further, standardization of image acquisition was achieved by onsite training. Lastly, image analysis was performed centrally with stringent quality control. These efforts achieved the goal of acquiring accurate and reproducible quantitative relaxation time values from each site and to enable pooling the data from all sites.

The longitudinal phantom $T_{1\rho}$ and T_2 RMS-CVs from each site are comparable to previous multi-site T_2 studies (17), indicating good longitudinal stability. The overall scan/re-scans RMS-CV in human subjects (3.1% for $T_{1\rho}$ and 4.0% for T_2) was comparable to single-site CVs (24–26) and better than a multi-site study (19). These CVs were less than the group differences between healthy and OA cartilage relaxation times, with a CV of 9–10% between the two groups (8). Our good multi-site *in vivo* reproducibility is attributed to our stringent study design.

Significant differences were observed for phantom $T_{1\rho}$ and T_2 values between the three sites and are attributed to different performances of the MR systems and RF coils as well as environmental influences. The phantom $T_{1\rho}$ and T_2 values between sites were highly correlated ($R > 0.99$), suggesting the differences maybe corrected and allow pooling data for multi-site analysis.

No significant differences were observed for *in vivo* $T_{1\rho}$ and T_2 values for the traveling control subjects between the three sites despite the significant differences in phantoms values. The differences maybe due to different coil loading between phantom and human subjects, and the small systematic differences between sites maybe masked by *in vivo* measurement variations. No significant differences in $T_{1\rho}$ and T_2 values were found in the traveling controls from baseline to follow-up, and the longitudinal CVs were comparable to cross-sectional CVs, suggesting good *in vivo* longitudinal reproducibility. This study is limited by the small number of human subjects for the cross-validation of $T_{1\rho}$ and T_2 between sites. In addition, the relatively low resolution of $T_{1\rho}$ and T_2 images (0.6 mm in plane with 4 mm slices) may introduce bias to $T_{1\rho}$ and T_2 values due to the partial volume effect. Advanced acceleration techniques can be applied in the future to obtain $T_{1\rho}$ and T_2 images with higher resolutions within clinically acceptable acquisition time (27). The reproducibility was evaluated only in healthy controls and should be evaluated in OA subjects in future studies. Different fitting methods generate significantly different quantification values (28, 29), and have different sensitivity to SNR and may yield different bias between MR systems or spatially across coils, which was not discussed in this study because the data were processed centrally using the same fitting method. Segmentation also introduces variation (30). The intra- and inter-operator variation using the same the post-processing software have been previously reported (31).

In conclusion, minimizing variation has enabled good reproducibility and cross-validation to be achieved between sites for cartilage $T_{1\rho}$ and T_2 quantification. This is an essential step prior to initiating multi-site longitudinal studies or clinical trials. The results from this study identify quality control and cross-calibration methods required for quantitative MRI to be applied in multi-site studies for evaluating cartilage degeneration. Future studies are needed to expand the multi-site study to include MR systems from multiple manufacturers.

Acknowledgments

The study was supported by NIH/NIAMS P50 AR060752 and the Arthritis Foundation (AF). The authors would like to thank the AF multi-site ACL study team.

References

1. Murphy L, Schwartz TA, Helmick CG, Renner JB, Tudor G, Koch G, et al. Lifetime risk of symptomatic knee osteoarthritis. Arthritis Rheum. 2008; 59(9):1207–13.10.1002/art.24021 [PubMed: 18759314]
2. Helmick C, Felson D, Lawrence R, Gabriel S, Hirsch R, Kwoh C, et al. Estimates of the prevalence of arthritis and other rheumatic conditions in the United States. Part I. Arthritis Rheum. 2008; 58(1): 15–25. [PubMed: 18163481]
3. Murray CJ, Vos T, Lozano R, Naghavi M, Flaxman AD, Michaud C, et al. Disability-adjusted life years (DALYs) for 291 diseases and injuries in 21 regions, 1990–2010: a systematic analysis for the Global Burden of Disease Study 2010. Lancet. 2012; 380(9859):2197–223.10.1016/S0140-6736(12)61689-4 [PubMed: 23245608]
4. Li X, Majumdar S. Quantitative MRI of articular cartilage and its clinical applications. J Magn Reson Imaging. 2013; 38(5):991–1008.10.1002/jmri.24313 [PubMed: 24115571]
5. Matzat SJ, van Tiel J, Gold GE, Oei EH. Quantitative MRI techniques of cartilage composition. Quantitative imaging in medicine and surgery. 2013; 3(3):162–74.10.3978/j.issn.2223-4292.2013.06.04 [PubMed: 23833729]

6. Link TM, Stahl R, Woertler K. Cartilage imaging: motivation, techniques, current and future significance. Eur Radiol. 2007; 17(5):1135–46.10.1007/s00330-006-0453-5 [PubMed: 17093967]
7. Potter HG, Black BR, Chong le R. New techniques in articular cartilage imaging. Clin Sports Med. 2009; 28(1):77–94.10.1016/j.csm.2008.08.004 [PubMed: 19064167]
8. Li X, Ma C, Link T, Castillo D, Blumenkrantz G, Lozano J, et al. In vivo T1rho and T2 mapping of articular cartilage in osteoarthritis of the knee using 3 Tesla MRI. Osteoarthritis and Cartilage. 2007; 15(7):789–97. [PubMed: 17307365]
9. Potter HG, Jain SK, Ma Y, Black BR, Fung S, Lyman S. Cartilage injury after acute, isolated anterior cruciate ligament tear: immediate and longitudinal effect with clinical/MRI follow-up. Am J Sports Med. 2012; 40(2):276–85. Epub 2011/09/29. 10.1177/0363546511423380 [PubMed: 21952715]
10. Mosher T, Dardzinski B. Cartilage MRI T2 relaxation time mapping: overview and applications. Seminars in musculoskeletal radiology. 2004; 8(4):355–68. [PubMed: 15643574]
11. Trattnig S, Domayer S, Welsch GW, Mosher T, Eckstein F. MR imaging of cartilage and its repair in the knee--a review. Eur Radiol. 2009; 19(7):1582–94. Epub 2009/03/14. 10.1007/s00330-009-1352-3 [PubMed: 19283387]
12. Liebl H, Joseph G, Nevitt MC, Singh N, Heilmeier U, Subburaj K, et al. Early T2 changes predict onset of radiographic knee osteoarthritis: data from the osteoarthritis initiative. Ann Rheum Dis. 201410.1136/annrheumdis-2013-204157
13. Bolbos R, Zuo J, Banerjee S, Link T, Ma C, Li X, et al. Relationship between trabecular bone structure and articular cartilage morphology and relaxation times in early OA of the knee joint using parallel MRI at 3 T. Osteoarthritis Cartilage. 2008; 16(10):1150–9. [PubMed: 18387828]
14. Regatte RR, Akella SV, Wheaton AJ, Lech G, Borthakur A, Kneeland JB, et al. 3D-T1rho-relaxation mapping of articular cartilage: in vivo assessment of early degenerative changes in symptomatic osteoarthritic subjects. Academic radiology. 2004; 11(7):741–9. [PubMed: 15217591]
15. Stahl R, Luke A, Li X, Carballido-Gamio J, Ma CB, Majumdar S, et al. T1rho, T2 and focal knee cartilage abnormalities in physically active and sedentary healthy subjects versus early OA patients--a 3.0-Tesla MRI study. Eur Radiol. 2009; 19(1):132–43. Epub 2008/08/19. 10.1007/s00330-008-1107-6 [PubMed: 18709373]
16. Su F, Hilton JF, Nardo L, Wu S, Liang F, Link TM, et al. Cartilage morphology and T1rho and T2 quantification in ACL-reconstructed knees: a 2-year follow-up. Osteoarthritis Cartilage. 2013; 21(8):1058–67.10.1016/j.joca.2013.05.010 [PubMed: 23707754]
17. Schneider E, Nessaiver M. The Osteoarthritis Initiative (OAI) magnetic resonance imaging quality assurance update. Osteoarthritis Cartilage. 2013; 21(1):110–6.10.1016/j.joca.2012.10.011 [PubMed: 23092792]
18. Schneider E, NessAiver M, White D, Purdy D, Martin L, Fanella L, et al. The osteoarthritis initiative (OAI) magnetic resonance imaging quality assurance methods and results. Osteoarthritis Cartilage. 2008; 16(9):994–1004.10.1016/j.joca.2008.02.010 [PubMed: 18424108]
19. Mosher TJ, Zhang Z, Reddy R, Boudhar S, Milestone BN, Morrison WB, et al. Knee articular cartilage damage in osteoarthritis: analysis of MR image biomarker reproducibility in ACRIN-PA 4001 multicenter trial. Radiology. 2011; 258(3):832–42. Epub 2011/01/08. [PubMed: 21212364]
20. Li X, Wyatt C, Rivoire J, Han E, Chen W, Schooler J, et al. Simultaneous acquisition of T1rho and T2 quantification in knee cartilage: repeatability and diurnal variation. J Magn Reson Imaging. 2014; 39(5):1287–93.10.1002/jmri.24253 [PubMed: 23897756]
21. Carballido-Gamio J, Bauer JS, RS, Lee KY, Krause S, Link TM, et al. Inter-subject comparison of MRI knee cartilage thickness. Medical Image Analysis. 2007; 12(2):120–35. [PubMed: 17923429]
22. Dardzinski BJ, Schneider E. Radiofrequency (RF) coil impacts the value and reproducibility of cartilage spin-spin (T2) relaxation time measurements. Osteoarthritis Cartilage. 2013; 21(5):710–20.10.1016/j.joca.2013.01.006 [PubMed: 23376528]
23. Pai A, Li X, Majumdar S. A comparative study at 3 T of sequence dependence of T2 quantitation in the knee. Magn Reson Imaging. 2008; 26(9):1215–20. [PubMed: 18502073]

24. Li X, Han E, Busse R, Majumdar S. In vivo T1rho mapping in cartilage using 3D magnetization-prepared angle-modulated partitioned k-space spoiled gradient echo snapshots (3D MAPSS). Magn Reson Med. 2008; 59(2):298–307. [PubMed: 18228578]
25. Pakin S, Schweitzer M, Regatte R. Rapid 3D-T1rho mapping of the knee joint at 3.0T with parallel imaging. Magn Reson Med. 2006; 56(3):563–71. [PubMed: 16894582]
26. Glaser C, Mendlik T, Dinges J, Weber J, Stahl R, Trumm C, et al. Global and regional reproducibility of T2 relaxation time measurements in human patellar cartilage. Magn Reson Med. 2006; 56(3):527–34.10.1002/mrm.21005 [PubMed: 16894587]
27. Zhou Y, Pandit P, Pedoia V, Rivoire J, Wang Y, Liang D, et al. Accelerating t cartilage imaging using compressed sensing with iterative locally adapted support detection and JSENSE. Magn Reson Med. 201510.1002/mrm.25773
28. Raya JG, Dietrich O, Horng A, Weber J, Reiser MF, Glaser C. T2 measurement in articular cartilage: impact of the fitting method on accuracy and precision at low SNR. Magn Reson Med. 2010; 63(1):181–93.10.1002/mrm.22178 [PubMed: 19859960]
29. Koff MF, Amrami KK, Felmlee JP, Kaufman KR. Bias of cartilage T2 values related to method of calculation. Magn Reson Imaging. 2008; 26(9):1236–43. Epub 2008/05/10. [PubMed: 18467063]
30. Koff MF, Parratte S, Amrami KK, Kaufman KR. Examiner repeatability of patellar cartilage T2 values. Magn Reson Imaging. 2009; 27(1):131–6. Epub 2008/09/20. [PubMed: 18801631]
31. Gupta R, Virayavanich W, Kuo D, Su F, Link TM, Ma CB, et al. MR T1ρ quantification of cartilage focal lesions in acutely injured knees: correlation with arthroscopic evaluation. Magn Reson Imaging. 2014 Epub ahead of print.

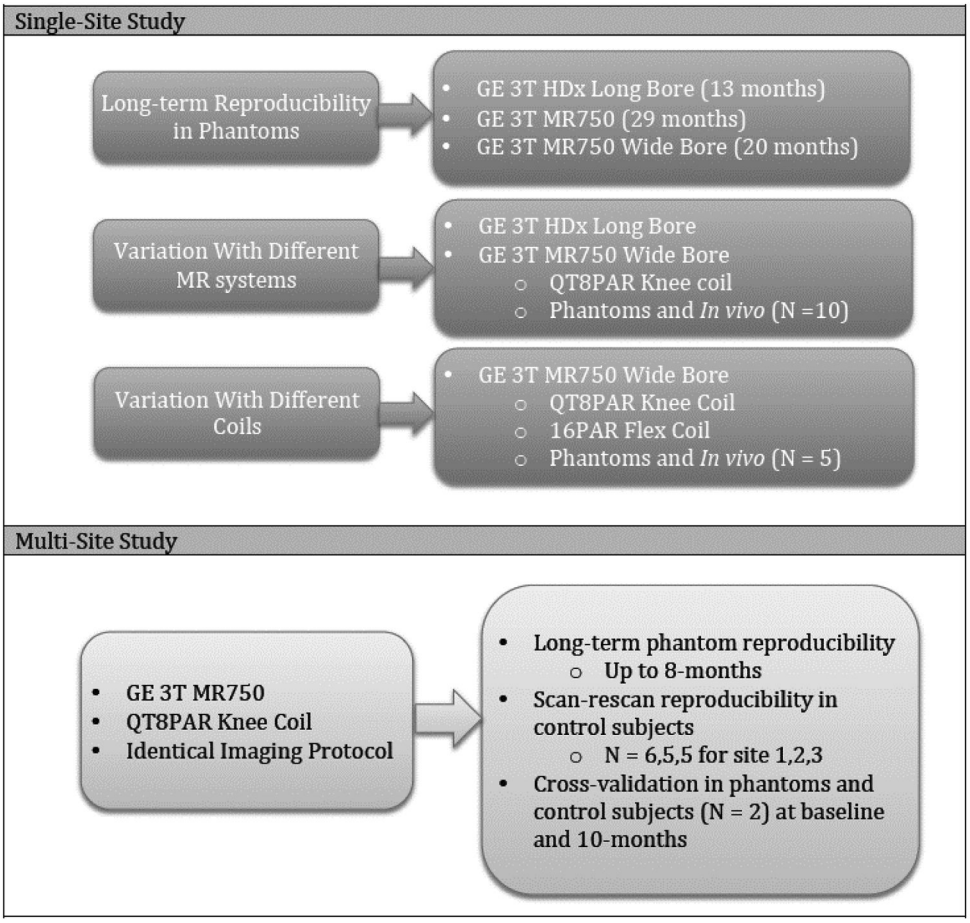

Figure 1.
Flow chart of the single-site and multi-site studies.

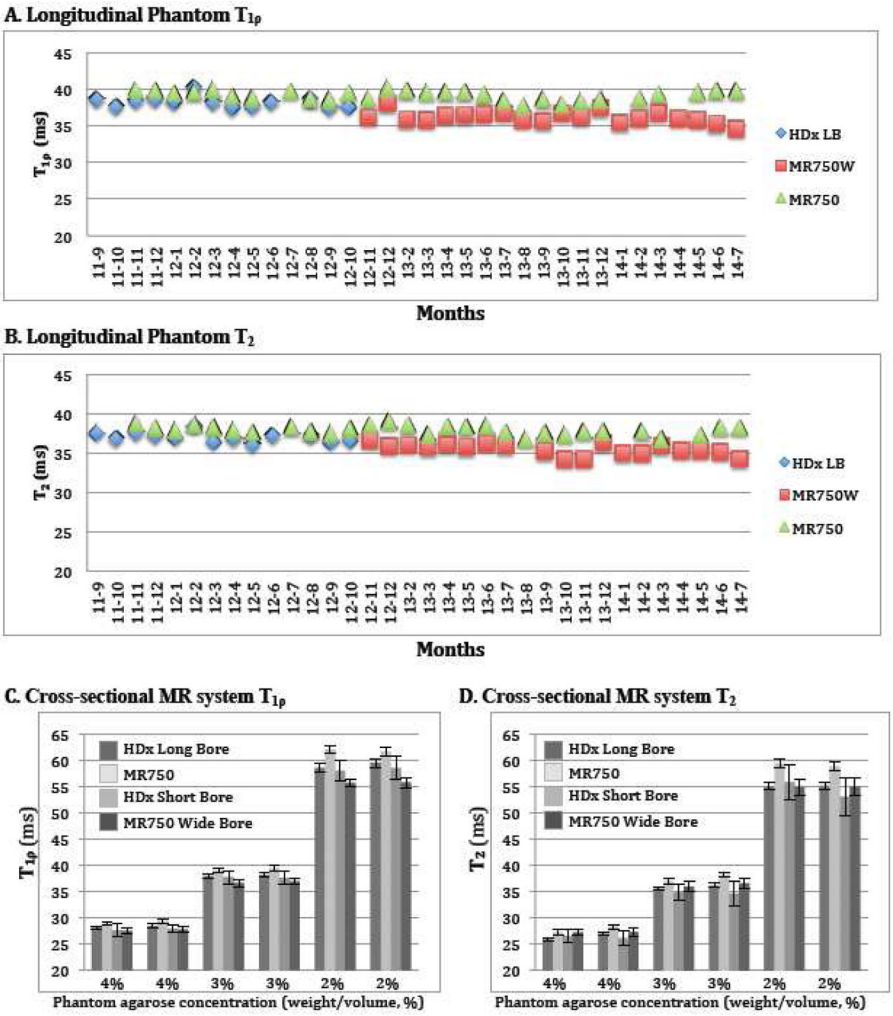

Figure 2.

Longitudinal reproducibility of $T_{1\rho}$ **(A)** and T_2 **(B)** values in a phantom with 3% agarose (weight/volume, %) measured from September 2011 (11–9) through July 2014 (14–7) using GE 3T MR systems: HDx long bore (HDx LB), MR750 wide bore (MR750W) and MR750. Cross-sectional variations in $T_{1\rho}$ **(C)** and T_2 **(D)** values in phantoms using four different models of GE 3T MR systems.

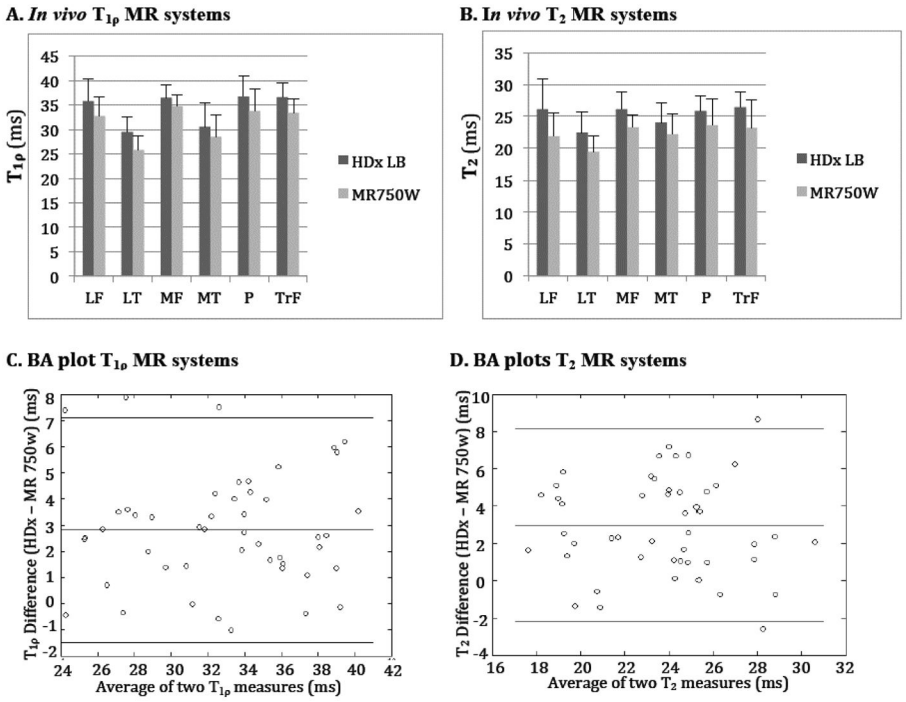

Figure 3.

Variations in *in vivo* $T_{1\rho}$ **(A)** and T_2 **(B)** values and Bland-Altman plots of $T_{1\rho}$ **(C)** and T_2 **(D)** values using different MR systems. $T_{1\rho}$ and T_2 measured using the HDx Long Bore were significantly higher than those measured using the MR750 wide bore.

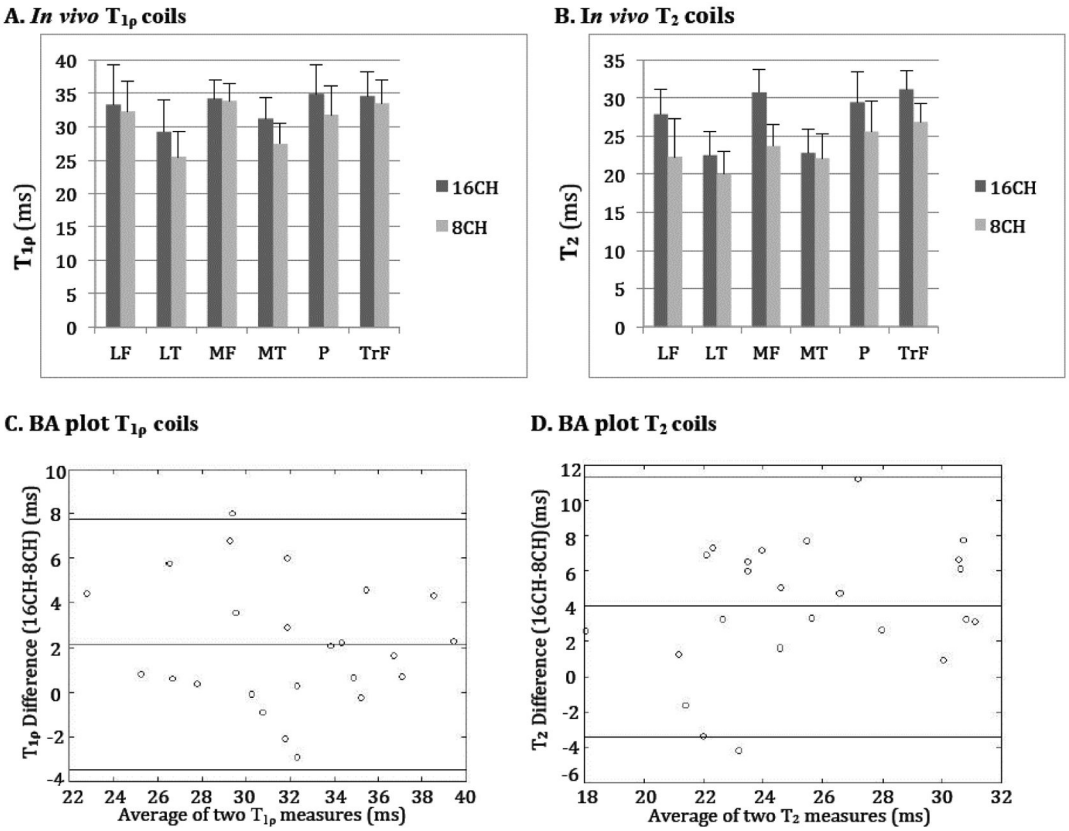

Figure 4.

Variations in *in vivo* $T_{1\rho}$ **(A)** and T_2 **(B)** values and Bland-Altman plots of $T_{1\rho}$ **(C)** and T_2 **(D)** values using different coils. $T_{1\rho}$ and T_2 measured using the 16PAR flex coil were significantly higher than those measured using the QT8PAR knee coil.

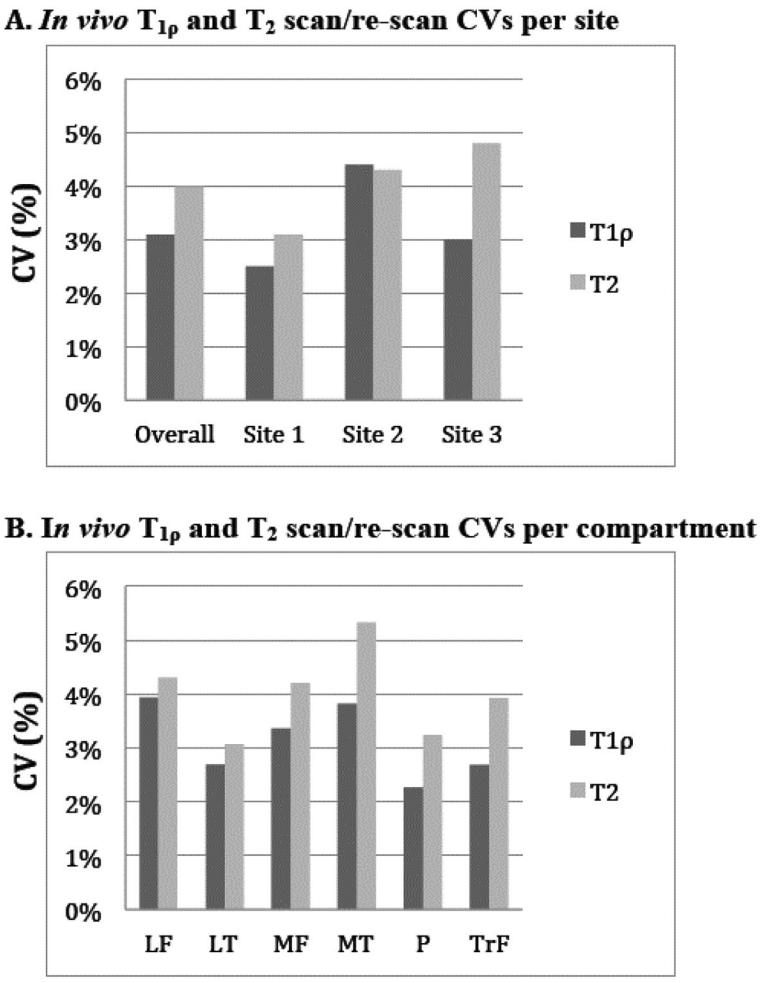

Figure 5.

In vivo scan/re-scan reproducibility of cartilage $T_{1\rho}$ and T_2 values of the multi-center study. **(A)** Overall CVs and CVs for each site; **(B)** CVs for each compartment.

Table 1

Imaging Protocols. Phantom protocols only included the 3D $T_{1\rho}$ and T_2 sequence; Human subject protocols included all sequences.

(A) Single-site Study								
Sequence	**TR/TE (ms)**	**ETL**	**FOV (cm)**	**Matrix**	**Slice thickness**	**NEX**	**Acceleration**	**Bandwidth (KHz)**
SAG fat-saturated 3D FSE (CUBE)	1500/25	50	14	384×384	1 mm	0.5	ARC Phase AF=2	50
SAG 3D $T_{1\rho}$ and T_2	7–9/min Full	-	14	256×128	4 mm	1	ARC Phase AF=2	64.5
Other parameters for $T_{1\rho}$ and T_2	Views Per Segment = 64, time of recovery = 1.2 s $T_{1\rho}$: time of spin-lock = 0/2/4/8/12/20/40/80 or 0/10/40/80 ms; spin-lock frequency = 500 Hz T_2: Preparation TE =0/1.6/3.2/6.5/12.9/25.9/38.8/51.8 or 0/13.7/27.3/54.7 ms							

(B) Multi-site Study								
Sequence	**TR/TE (ms)**	**ETL**	**FOV (cm)**	**Matrix**	**Slice thickness**	**NEX**	**Acceleration**	**Bandwidth (KHz)**
Sagittal fat-saturated T_2w FSE	5000/40	16	16	320×224	3.5 mm (gap=0)	1	ASSET AF=2	41.67
Sagittal/Coronal/Axial PDw FSE	5100/30	16	13	512 × 480	3.5 mm (gap=0)	1	ASSET AF=2	62.5
Sagittal fat-saturated 3D FSE (CUBE)	1500/25	50	14	384×384	1 mm	0.5	ARC Phase AF=2	50
Sagittal 3D $T_{1\rho}$ and T_2	7–9/min Full	-	14	256×128	4 mm	1	ARC Phase AF=2	64.5
Other parameters of $T_{1\rho}$ and T_2	Views Per Segment = 64, time of recovery = 1.2 s $T_{1\rho}$: time of spin-lock = 0/10/40/80 ms; spin-lock frequency = 500 Hz T_2: Preparation TE =2.9/13.6/24.3/45.6 ms							

Table 2

RMS-CV of longitudinal $T_{1\rho}$ and T_2 values at the center, left and right positions.

(A) For each MR system in the single-site study				
Mean RMS-CV (%)		**HDx long bore**	**MR750**	**MR750 wide bore**
$T_{1\rho}$	Center	1.8%	2.0%	2.1%
	Left	2.0%	2.4%	2.4%
	Right	2.3%	2.7%	2.5%
T_2	Center	2.3%	2.5%	2.8%
	Left	1.8%	1.8%	2.3%
	Right	1.7%	2.1%	1.9%

(B) For each site in the multi-center study				
Mean RMS-CV (%)		**Site 1**	**Site 2**	**Site 3**
$T_{1\rho}$	Center	1.8%	2.3%	1.5%
	Left	2.0%	2.6%	1.6%
	Right	2.2%	2.6%	1.3%
T_2	Center	2.1%	2.7%	1.8%
	Left	1.2%	2.4%	1.2%
	Right	2.0%	2.3%	1.3%

Osteoarthritis Cartilage. Author manuscript; available in PMC 2016 December 01.

Table 3

Mean and SD, fitting errors, pooled RMS of inter-location variations, short-term and long-term reproducibility, and pooled RMS with different MR systems, coils and sites of $T_{1\rho}$ and T_2 values.

$T_{1\rho}$ Phantoms									
Agarose Concentration (weight/volume, %)	**Average # of Voxels Within ROI (n=52)**	**Mean $T_{1\rho}$ (ms) (n=52)**	**Pooled SD (ms) within ROI (n=52)**	**Normalized RMS Fitting Error (n=52)**	**Pooled RMS (ms) of Inter-location Variation (n=52)**	**Pooled RMS (ms) of Long-term Reproducibility (n=52)**	**Pooled RMS (ms) with Different MR Systems (n=2)**	**Pooled RMS (ms) with Different Coils (n=2)**	**Pooled RMS (ms) with Different Sites (n=2)**
4%	5390	28.1	1.1	0.0056	0.5	0.6	0.4	0.4	0.9
3%	5390	37.9	1.2	0.0056	0.4	0.7	0.9	0.5	1.1
2%	5390	58.8	1.8	0.0050	0.4	1.2	2.3	1.1	1.9
$T_{1\rho}$ Human Subjects									
Cartilage Compartment	Average # of Voxels Within ROI (n=16)	Mean $T_{1\rho}$ (ms) (n=16)	Pooled SD (ms) within ROI (n=16)	Normalized RMS Fitting Error (n=16)	Pooled RMS (ms) of Short-term Scan/ rescan Reproducibility (n=16)	Pooled RMS (ms) of Long-term Reproducibility (n=4)	Pooled RMS (ms) with Different MR Systems (n=10)	Pooled RMS (ms) with Different Coils (n=5)	Pooled RMS (ms) with Different Sites (n=4)
LF	2693	45.5	11.8	0.009	1.7	1.6	1.5	2.1	1.7
LT	1778	39.5	10.2	0.013	1.0	1.0	2.0	3.3	1.6
MF	3981	44.9	10.6	0.006	1.5	1.2	2.3	3.8	1.9
MT	1871	39.0	12.9	0.014	1.5	1.5	1.7	2.6	1.7
P	1739	46.9	9.4	0.013	1.1	1.7	2.3	1.4	2.3
TrF	2764	46.5	9.5	0.008	1.2	2.1	1.9	1.6	2.6
T_2 Phantoms									
Agarose Concentration (weight/volume, %)	Average # of Voxels Within ROI (n=52)	Mean T_2 (ms) (n=52)	Pooled SD (ms) within ROI (n=52)	Normalized RMS Fitting Error (n=52)	Pooled RMS (ms) of Inter-location Variation (n=52)	Pooled RMS (ms) of Long-term Reproducibility (n=52)	Pooled RMS (ms) with Different MR Systems (n=2)	Pooled RMS (ms) with Different Coils (n=2)	Pooled RMS (ms) with Different Sites (n=2)
4%	5390	27.2	0.8	0.0056	0.5	0.7	0.1	0.6	1.1
3%	5390	36.4	1.0	0.0069	0.5	0.8	0.3	1.2	1.5
2%	5390	56.0	1.8	0.0061	1.2	1.6	0.5	1.8	2.6
T_2 Human Subjects									

$T_{1\rho}$ Phantoms									
Agarose Concentration (weight/volume, %)	**Average # of Voxels Within ROI (n=52)**	**Mean $T_{1\rho}$ (ms) (n=52)**	**Pooled SD (ms) within ROI (n=52)**	**Normalized RMS Fitting Error (n=52)**	**Pooled RMS (ms) of Inter-location Variation (n=52)**	**Pooled RMS (ms) of Long-term Reproducibility (n=52)**	**Pooled RMS (ms) with Different MR Systems (n=2)**	**Pooled RMS (ms) with Different Coils (n=2)**	**Pooled RMS (ms) with Different Sites (n=2)**
Cartilage Compartment	Average # of Voxels Within ROI (n=16)	Mean T_2 (ms) (n=16)	Pooled SD (ms) within ROI (n=16)	Normalized RMS Fitting Error (n=16)	Pooled RMS (ms) of Short-term Scan/ rescan Reproducibility (n=16)	Pooled RMS (ms) of Long-term Reproducibility (n=4)	Pooled RMS (ms) with Different MR Systems (n=10)	Pooled RMS (ms) with Different Coils (n=5)	Pooled RMS (ms) with Different Sites (n=4)
LF	2693	32.7	9.7	0.014	1.4	1.3	2.5	0.2	1.2
LT	1778	28.3	8.6	0.012	0.8	0.8	2.6	2.2	1.3
MF	3981	32.3	8.9	0.012	1.4	1.6	1.8	1.8	0.9
MT	1871	29.5	9.7	0.012	1.5	1.5	2.1	1.4	1.2
P	1739	31.9	7.3	0.009	1.0	1.4	2.0	0.2	1.5
TrF	2764	34.4	9.2	0.011	1.3	1.3	2.7	0.7	1.5

Table 4

SNR of control knees using different MR systems and different coils

Images		LF	LT	MF	MT	P	TrF
TSL/TE=0	HDx LB (8Ch)	48.7±12.3	43.2±10.6	51.9±11.3	45.5±11.2	77.2±19.2	65.9±11.1
	MR750W (8Ch)	43.8±15.5	31.5±17.9	47.9±17.0	32.9±20.0	54.6±17.3	48.6±13.1
	MR750W (16Ch)	67.6±21.4	58.8±19.8	74.6±20.2	61.5±19.5	70.6±20.2	73.4±26.0
TSL = 80ms	HDx LB (8Ch)	11.4±1.5	10.8±2.4	12.3±3.2	12.8±2.6	14.5±5.3	17.4±2.8
	MR750W (8Ch)	8.2±0.4	7.7±2.6	8.5±1.0	7.5±3.2	11.7±1.6	11.6±2.6
	MR750W (16Ch)	13.0±4.0	9.4±3.7	13.7±4.7	12.2±4.8	12.3±4.5	17.9±7.3
TE = 54.7ms	HDx LB (8Ch)	11.6±2.6	12.6±3.1	15.5±4.2	15.3±4.2	15.3±5.0	21.1±3.4
	MR750W (8Ch)	8.8±2.0	9.5±2.4	9.8±2.3	9.1±2.3	11.7±2.9	14.4±3.6
	MR750W (16Ch)	12.7±3.3	11.5±5.9	14.7±6.3	14.1±7.1	12.5±6.4	18.8±7.9

8Ch: Quadrature transmit and 8-channel phased array receive knee coil; 16Ch: receive only 16-channel phased array flex coil.